Physical Science International Journal

24(2): 1-20, 2020; Article no.PSIJ.55149
ISSN: 2348-0130

The Pause End and Major Temperature Impacts during Super El Niños are Due to Shortwave Radiation Anomalies

Antero Ollila[1*]

[1]Department of Civil and Environmental Engineering (Emer.), School of Engineering, Aalto University, Espoo, Otakaari 1, Box 11000, 00076 Aalto, Finland.

Author's contribution

The sole author designed, analyzed, interpreted and prepared the manuscript.

Article Information

DOI: 10.9734/PSIJ/2020/v24i230174
Editor(s):
(1) Dr. Pratima Parashar Pandey, College of Engineering and Technology, Integrated Institutes of Learning, Dr. A.P.J. Abdul Kalam Technical University, India.
(2) Dr. Roberto Oscar Aquilano, National University of Rosario (UNR), Physics Institute of Rosario (IFIR) (CONICET-UNR), Argentina.
Reviewers:
(1) Elisha Akech Ochungo, University of Nairobi, Kenya.
(2) Agu Eensaar, Tallinn University of Applied Sciences, Estonia.
(3) Germana Arruda de Queiroz, Brazil.
Complete Peer review History: http://www.sdiarticle4.com/review-history/55149

Original Research Article

Received 29 December 2019
Accepted 05 March 2020
Published 13 March 2020

ABSTRACT

The hiatus or temperature pause during the 21st century has been the subject of numerous research studies with very different results and proposals. In this study, two simple climate models have been applied to test the causes of global temperature changes. The climate change factors have been shortwave (SW) radiation changes, changes in cloudiness and ENSO (El Niño Southern Oscillation) events assessed as the ONI (Oceanic Niño Index) values and anthropogenic climate drivers. The results show that a simple climate model assuming no positive water feedback follows the satellite temperature changes very well, the mean absolute error (MAE) during the period from 2001 to July 2019 being 0.073°C and 0.082°C in respect to GISTEMP. The IPCC's simple climate model shows for the same period errors of 0.191°C and 0.128°C respectively. The temperature in 2017-2018 was about 0.2°C above the average value in 2002–2014. The conclusion is that the pause was over after 2014 and the SW anomaly forcing was the major reason for this temperature increase. SW anomalies have had their greatest impacts on the global temperature during very strong (super) El Niño events in 1997-98 and 2015-16, providing a new perspective for ENSO events. A positive SW anomaly continued after 2015-16 which may explain the weak La Niña 2016

**Corresponding author: E-mail: aveollila@yahoo.com;*

temperature impacts, and a negative SW anomaly after 1997-98 may have contributed two strong La Niña peaks 1998-2001. No cause and effect connection could be found between the SW radiation and temperature anomalies in Nino areas.

Keywords: Pause; hiatus; climate change; ENSO; El Niño; shortwave changes.

1. INTRODUCTION

During the 21st century, global surface mean temperature (GSMT) change has hardly increased, thus deviating from the climate models applied by the IPCC. This phenomenon has been called "a global warming hiatus" or "a temperature pause" or "a slowdown." In this study, the term "pause" has been used. Debate among the climate community has resulted in more than 200 research studies in some cases with opposite results for why the pause occurred. The underlying question is the anthropogenic warming, which seems to disappear during the pause even though the concentrations of greenhouse (GH) gases have been steadily growing.

Knight [1] and Fyfe et al. [2] have shown that the pause is real, and Otto et al. [3] and Fyfe et al. [4] have concluded that climate sensitivity has decreased. There is a group of studies [5-12] that approve the existence of the pause, but the GSMT is inside the lower end of the uncertainty limits of the IPCC's climate models. The reasons for the pause according to these studies are variations in solar inputs, volcanic inputs, amounts of aerosols and ENSO events.

Many research studies [13-21] have concluded that the warming has continued as predicted by climate models, but the heat has been absorbed into the oceanic heat sink. Cheng et al. [22] have found that the opposite phenomenon happens, because there is a strong negative ocean heat content tendency in the tropical Pacific Ocean during El Niño. The high sea surface temperatures drive enhanced air-sea heat fluxes into the atmosphere. This proposal can be criticized because the surface water warms up and the underlying subsurface water stays cool due to weakened mixing effect in the mixing layer.

Some studies [17,22,23] show that Pacific Decadal Oscillation (PDO) has cooled the atmosphere. The PDO index indicates cooling since about 2000 and at about 2014, it turned into warming [24]. Atlantic Multidecadal Oscillation (AMO) has been in warming mode since 2000 [25]. Other proposed reasons for the pause have been a prolonged solar minimum [26] and tropospheric or stratospheric water vapor [27-29].

Obviously, the largest number of studies has concluded that there is no pause based on statistical analyses or other analyses of temperature measurements [30-39].

Trenberth et al. [40] examined the results of the complicated three-dimensional Community Earth System Model (CESM) with respect to the observations from 2000–2014. They found that the model calculated GSTM increase of 0.4°C was significantly greater than the observed 0.12°C, and the ENSO events' magnitude was about 40% greater than observed. They concluded that the temperature pause was still a reality at the end of 2015.

Scafetta et al. [41] have shown that the temperature peak in 2015–16 is unrelated to anthropogenic forcing, and it is simply associated with the ENSO phenomenon. The researchers removed the ENSO signature from the 2000 to 2016 trend, and thereafter, GCM (General Circulation Model) simulations diverged from the observations. The authors concluded that the GCMs used to support the AGWT (Anthropogenic Global Warming Theory) are very likely flawed.

Yin et al. [42] have proposed that the high temperatures of 2014-2016 were due to the long-term increase of GH gases and the super El Niño event releasing unusually large amounts of ocean heat from the subsurface layer of the northwestern tropical Pacific. These proposals can be criticized on the following grounds: 1) The warming effects of GH gases happen according to the time delays of ocean (3 months) and land (1 month), preventing accumulation effects. 2) A common explanation for El Niño is the Walker circulation decrease, which eliminates the upwelling of cold seawater, causing the ocean surface water temperature to increase. This means that subsurface water cannot release more heat to the surface water, but it will cool down because there is not enough mixing with

warm surface water. On the other hand, during La Niña the mixing of surface water with colder subsurface water decreases the temperature. Because of these different mechanisms, El Niño's peak is typically higher than that of La Niña, and El Niño peak's duration is shorter than La Niña's peak.

The findings of the studies [40-42] show that the modelling of both the temperature pause and ENSO events still needs much better understanding. This conclusion is easy to accept based on the different and even conflicting conclusions of the research studies briefly referenced in this section.

Hedemann et al. [43] found out that energy flux deviations as small as 0.08 W m^{-2} originating at the top of the atmosphere and/or in the ocean could explain the hiatus. They suggested that the origin of the recent hiatus may never be identified. The apparent problem in their conclusion is that they restricted their analysis on the anthropogenic climate models excluding the cosmic forces. Despite this issue, the climate researchers have continued their research work on the pause and published research studies since spring 2017 at least at the same rate as earlier. This is quite natural because the pause is real, and the reasons are not generally accepted by the climate science community.

Loeb et al. [44] found a significant reduction of 0.83 ± 0.41 Wm^{-2} in global mean reflected SW flux at the top-of-atmosphere (TOA) flux during the years 2014-2017 after the pause resulting in an increase in net energy into the climate system. Decreases in low cloud cover were the primary driver of the decrease in reflected SW TOA flux.

Temperature data sets are not equal, and they show different warming values during the pause. Two used in this study are the UAH satellite temperature data set, developed by the University of Alabama in Huntsville [45] and GISTEMP of NASA Goddard's Global Surface Temperature Analysis, combining land surface air temperatures with sea surface temperatures [46]. The UAH temperature is the temperature of the lower troposphere and there is ongoing debate how well its changes is correlated to the surface temperature changes.

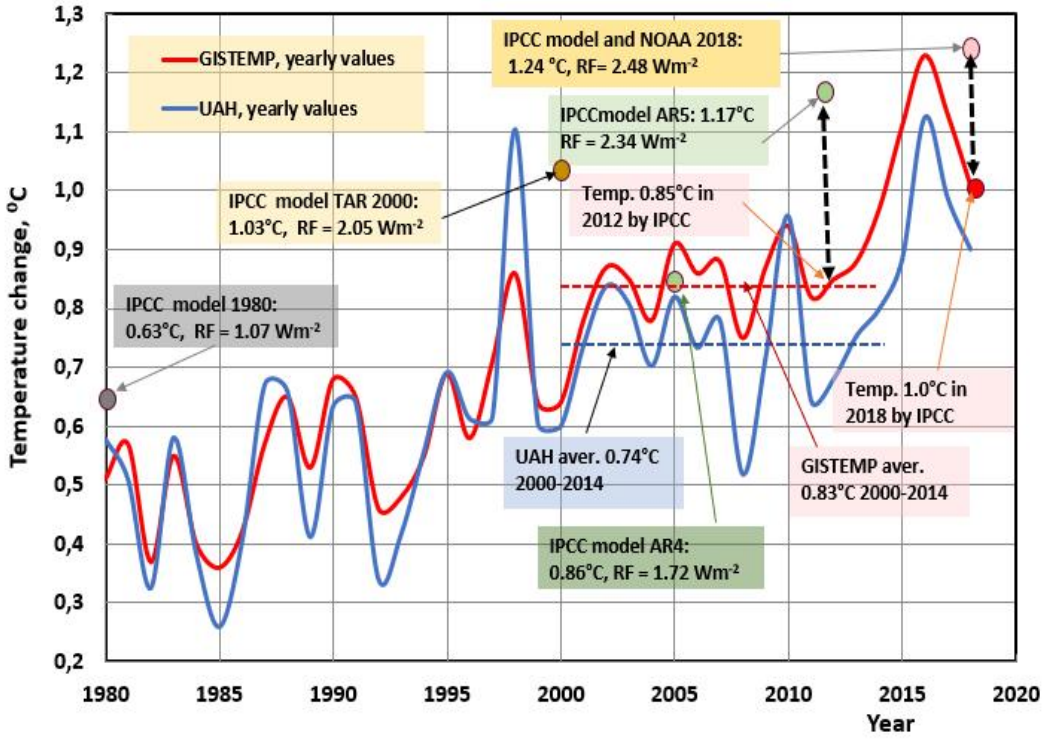

Fig. 1. Temperature trends and warming values of the IPCC

Both temperature curves are depicted in Fig. 1. The warming values of the IPCC have calculated according to assessment reports [47,48]. GISTEMP was normalized to be 0.85°C in 2012 as reported by the IPCC [48] (SPM, p.4) and the UAH was normalized to have the same average value as GISTEMP during 1979–1984.

The IPCC-reported model values in Fig. 1 are calculated using the climate sensitivity parameter λ value 0.5 K/(Wm^{-2}) according to IPCC [49] (chapter 6.2.1). The error in 2011 between the model calculated GSMT and the measured temperature was about 37%. Both temperature data sets closely follow each other from 1980 to 2000, but the UAH is more sensitive for ENSO event changes. GISTEMP started to deviate from the UAH in 2000, and it is now 0.1–0.2°C higher than the UAH. Research studies indicating "no pause" have normally used GISTEMP in their analyses. An increasing trend in GSMT can be noticed in Fig. 1, but this impression is caused mainly by the super El Niño of 2015-16. The GSMT had not yet returned to the average value during 2000–2014, and the reasons are analyzed in this study.

The mechanisms of ENSO events have not been fully understood and the reasons for ENSO magnitudes are still unclear. Hong et al. [50] have found that Southern Hemispheric transverse circulation is a prerequisite for extreme magnitude El Niño events.

The main objective of this study is to analyze the warming effects of shortwave (SW) irradiance changes, ENSO events, greenhouse gases and cloudiness changes during the pause and find out how well they can explain the measured GSMT variations. Two simple climate models have been applied in analyses. The results of climate models have used for analyzing the accuracies of the models and the reasons for the differences. In this study, the SW irradiance anomaly has been analyzed as a significant contributor to temperature effects of the super El Niño of 1997-98 and 2015-16.

2. MATERIALS AND METHODS

2.1 Materials

The author assesses [45] UAH (2018) as more reliable than the GISTEMP [46] data set for two reasons. Firstly, the UAH is based on satellite measurements evenly covering the whole globe, but GISTEMP is based on a sparse and unevenly distributed measurement network. Secondly, GISTEMP has been continuously updated according to new calculation methods, leading to a general observation that history is getting colder and that temperatures since 2000 have been getting warmer in comparison to older versions. IPCC's report AR4 [47] states: "*New analyses of balloon-borne and satellite measurements of lower- and mid-tropospheric temperature show warming rates that are similar to those of the surface temperature record and are consistent within their respective uncertainties, largely reconciling a discrepancy noted in the TAR*." TAR is the third assessment report of the IPCC [49].

The material for ENSO event analyses is the ONI provided by NOAA [51]. The Clouds and the Earth's Radiant Energy System (CERES) provides SW irradiance and longwave (LW) radiation fluxes from CERES satellite measurements maintained by NOAA [52]. The radiation fluxes before CERES are available from NASA's Earth Radiation Budget Experiment (ERBE) Research Program providing the Earth's radiation budget information. There is missing radiation data between the ERBE and CERES from August 1999 to December 2000, but this is not crucial in analyses. The absolute water humidity values are from the NOAA data set [53]. The radiative forcing (RF) values of greenhouse (GH) gases and drivers are from the IPCC's assessment reports [47-49]. The values after 2011 are from NOAA's annual greenhouse index [54].

The IPCC's total radiative forcing of AR4 [47] for 2005 is calculated in a different way than the other IPCC values, because its value differs so much from the values of TAR and AR5. It is not possible that anthropogenic climate forcing would be lower in 2005 than in 2000.

2.2 Methods

The methodology of this study is based on using two simple climate models for finding out the driving forces during the pause. The time interval is one month which necessitates using a dynamic approach. Statistical methods have been applied to analyzing the results. A simple radiative forcing concept has been applied as used by the IPCC [49] (p. 664) and thereafter in later reports [47,48] where the surface temperature response depends linearly on RF:

$$dT = \lambda * RF, \quad (1)$$

where dT is temperature change (°C or K), λ is the climate sensitivity parameter (K/(Wm^{-2}), and RF is radiative forcing (Wm^{-2}). This Eq. is applicable to GH gases as well as SW irradiance changes. Eq. (1) has been applied in both climate models in this study.

IPCC uses both ECS (Equilibrium Climate Sensitivity) and TCS (Transient Climate Sensitivity) concepts and summarizes the differences in AR5 [48], (p. 1110): "*ECS determines the eventual warming in response to stabilization of atmospheric composition on multi-century time scales, while TCR determines the warming expected at a given time following any steady increase in forcing over a 50- to 100-year time scale."* IPCC has changed the TCS to TCR (Transient Climate Response). On page 1112 of AR5 [48], IPCC states that "*TCR is a more informative indicator of future climate than ECS."* The TCS definition resumes that the Increase rate of CO_2 concentration is of maximum 1%y^{-1}. This condition is applicable during the pause.

Because the climate models applied in this study are very simple, a question could be raised, if they are accurate enough for calculating RF warming impacts. The Transient Climate Sensitivity (TCS) can be calculated using Eq. (1) with λ and RF values according to the IPCC choices (λ = 0.5 K/(Wm^2) and RF = 3.7 Wm^{-2}) which gives the value 1.85°C. In the IPCC's report AR5 [48] TCS is between 1.0°C to 2.5°C and it means the average value of 1.75°C. Two other TCS values can be found in the AR5 [48]. IPCC reports that "*It can be estimated that in the presence of water vapor, lapse rate and surface albedo feedbacks, but in the absence of cloud feedbacks, current GCMs would predict a climate sensitivity (±1 standard deviation) of roughly 1.9°C ± 0.15°C*." In Table 9.5 of AR5 [48] has been tabulated the key figures of 30 GCMs, and the model TCS average of these GCMs is 1.8°C. Ollila [55] has shown that Eq. (1) gives the same average temperature change values for CO_2 concentration from 280 ppm to 1370 ppm as the most complicated computer models in calculating RCP scenario responses..

In the TCS calculations, the dynamic effects are not needed to consider but during the pause, they should be included. The GSMT response for RF forcing at the TOA happens after dynamical delays. These system delays can be approximated by two parallel first-order dynamic transfer systems of ocean and land.

$$dT_{SW} = \lambda * RF * (K_{sea} * \exp(-t/T_{sea}) + K_{land} * \exp(-t/T_{land})) \quad (2)$$

where t is time (months), exp is exponent, K_{sea} is 0.7, K_{land} is 0.3, T_{sea} is a time constant of 2.74 months, and T_{land} is a time constant of 1.04 months. These values are based on the studies of [56-58]. The magnitude of time constants implies that the surface temperature has a settling time about one year to an RF change. This means that Eq.s (1) and (2) can be applied for interannual variability calculations. The values of the K parameters are the land and ocean area portions of the Earth.

The dynamic processes according to Eq. (3) are first-order dynamic models, which can be simulated in the discrete form, enabling continuously changing input variables:

$$dT_{SW}(n) = \Delta t/(T+\Delta t))/((T/\Delta t) * (Out(n-1) + In(n), \quad (3)$$

where Out(n) is the output of the process in step n, In(n) is the input of the process of step n, T is the time constant, Δt is the simulation step interval (1 month), and n-1 is the previous step value.

2.2.1 IPCC model

The temperature change of the "IPCC model" is a combination of three terms

$$dT = dT_{SW} + dT_{ENSO} + dT_{ANTR} \quad (4)$$

where dT_{SW} is the temperature impact of SW forcing, dT_{ENSO} is the ENSO temperature impacts and dT_{ANTR} is the temperature impact of anthropogenic RF factors. The calculation of dT_{SW} and dT_{ENSO} terms is explained later. In AR5 of the IPCC [48] the anthropogenic changes have the main role of 97.9 % contribution in long-term GSMT changes. It has been assumed that these terms are not essentially correlated with each other and therefore they can be summarized together. The IPCC [48] keeps the elements of Eq. (4) independent and they can be summarized for calculating the total RF and warming impact. This assumption will be analyzed later in Discussion section based on the calculated results.

The IPCC model, T_{ANTR} is the same as the total anthropogenic RF of the IPCC [48] including the GH gases, aerosols and cloud adjustments as well as the albedo changes due to land use. The solar irradiance changes are not included in

Eq. (4) because they are part of SW radiative forcing. The yearly values of anthropogenic RF-values have been calculated by the interpolation method from the assessment reports of the IPCC [47-49]. Because the total RF value of AR4 is an outlier, it has not been used but the yearly values have been interpolated from 2000 and 2011 values.

Both SW forcing and anthropogenic forcing effects have been calculated by a simple RF Eq. [48]

$$dT = 0.5 * RF \quad (5)$$

The λ value 0.5 K/(Wm^{-2}) means that positive water feedback has been applied, which is a common feature in climate models as defined by the IPCC in section 6.2.1 of [49] and in section 2.2 of [47].

2.2.2 Ollila model

In this study, an alternative climate model is called the "Ollila model", which is a combination of four different warming processes

$$dT = dT_{SW} + dT_{ENSO} + dT_{CLOUD} + dT_{GHG} \quad (6)$$

where dT_{CLOUD} is the temperature impacts of cloudiness changes, and the dT_{GHG} is the temperature impacts of GH gases.

In the "Ollila model" Eq. (1) has been applied but λ has a different value. The λ value is from Ollila's three studies [59-61] showing that there is no positive water feedback in the atmosphere. This result is based on the λ value calculated by two methods from the Earth's energy balance and from the spectral analysis calculations and λ value is 0.27 K/(Wm^{-2}).

Anthropogenic warming includes only carbon dioxide because during the pause methane and nitrogen oxide forcing impact changes are insignificant (< 0.001°C). In the Ollila model the radiative forcing of CO_2 is calculated according to the earlier research study [59]

$$dT_{GHG} = 0.27 * 3.12 * \ln (C/280) \quad (7)$$

where C is the actual concentration of CO_2 (ppm).

2.2.3 Shortwave forcing

There are two methods for calculating the RF effects of solar irradiance. The simplest way is to use only SW radiation changes at the TOA (top of the atmosphere). If the SW change or anomaly (=SW forcing) exists for a longer time, the surface temperature starts to increase, and it finally comes to a new balance value in about one year. An alternative method called "instantaneous change in net forcing", which is SW radiative flux down minus longwave (LW) radiative flux up at the TOA as defined by the IPCC [48] (ch. 8.1.1.1), and also used by Trenberth et al. [40]. The TOA in the CERES data sets is the climatological tropopause at the 20 km altitude because CERES radiation values have been adjusted for this altitude [52]. In this study the SW forcing method has been applied, because the LW radiation upwards depends strongly on the surface temperature, and this would cause the autocorrelation effect.

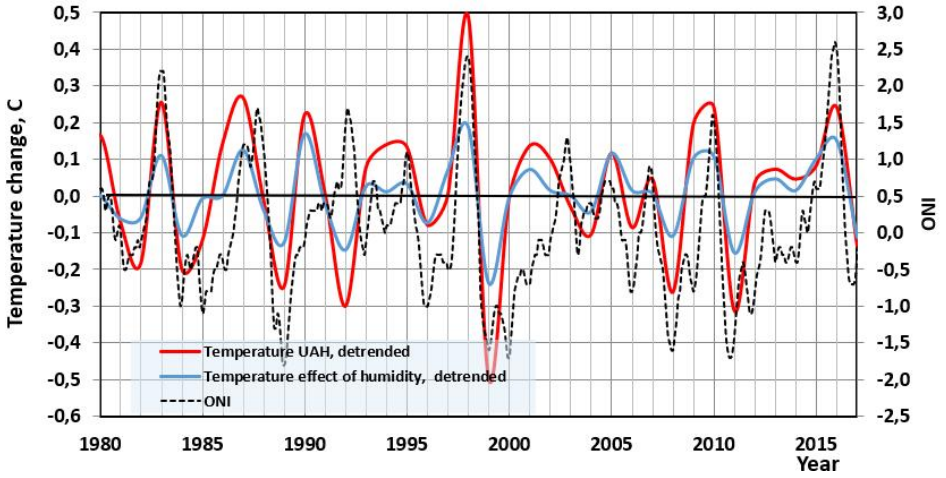

Fig. 2. ONI, detrended UAH temperature anomalies and detrended water vapor temperature trends on a Global scale

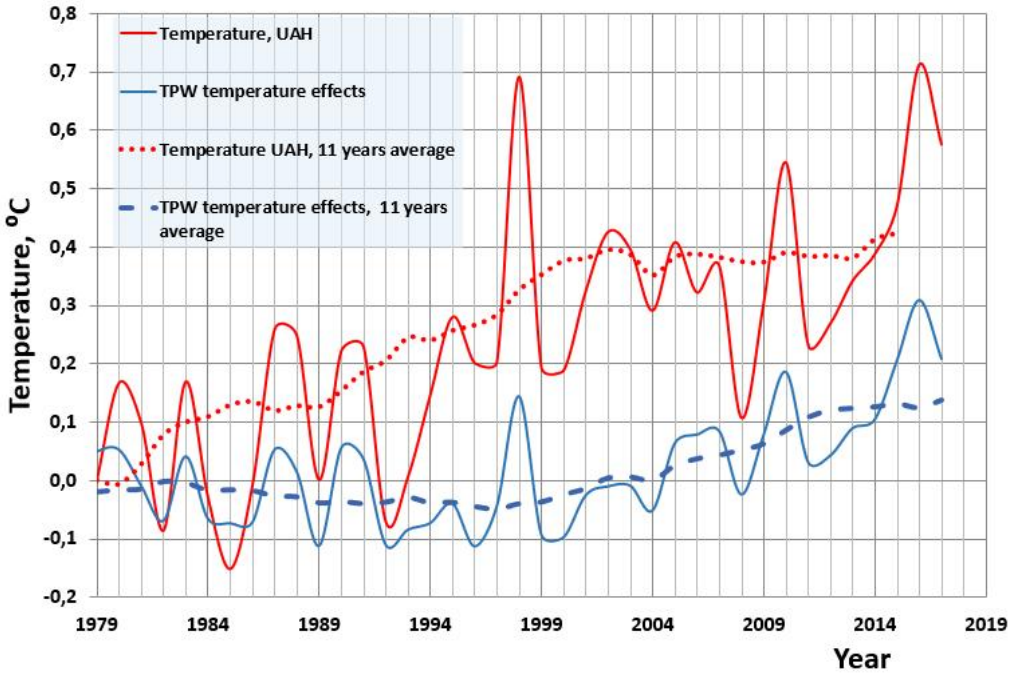

Fig. 3. Short- and long-term effects of water vapor on Global scale

2.2.4 The temperature impacts of ENSO events

The main reason for the global temperature effects of ENSO events seems to be the events' capability to change the absolute water vapor amount in the global atmosphere, as illustrated in Fig. 2.

The analyses depicted in Figs. 2 and 3 are started from the year 1979 by modifying temperature changes and all warming impacts to start from zero. The ENSO effect on temperature is abnormal from 1991 to 1993 because of the Mount Pinatubo eruption effects due to diffuse SW radiation [58]. The warming impacts of water are calculated based on the absorption calculations by increasing the water content of the average global atmosphere conditions (2.6 prcm / 305.978 Wm^{-2}) to the TPW (Total Precipitable Water) value of 2.856 prcm (prcm = precipitable water in centimeters) giving the absorption value of 306.709 Wm^{-2}. By forcing the warming value (T) in Celcius degrees to be zero in 1979, Eq. (8) could be concluded [60]:

$$dT = -6.797 + 2.81 * TPW, \quad (8)$$

By comparing the total temperature variations and the simultaneous water vapor effects, it is easy to conclude that water vapor plays an important role because its contribution to the ENSO temperature effect is about 50%. The positive temperature effect is based on the fact that water vapor as a GH gas is about 12 times stronger than CO_2 [59]. This is a perfect example that positive water feedback is a reality in short-term events like ENSO. The temperature and the absolute water vapor trend are depicted in Fig. 3 [60]. It can be noticed that for 1982–2003, the global temperature anomaly has been increasing but long-term water vapor amount has been decreasing. This observation does not confirm the assumption of most anthropogenic climate models that there is permanent positive water feedback in the atmosphere doubling the warming effects of GH gases. The correct theory works all the time in all defined conditions and not only occasionally.

Even though ENSO events are regional, they have global temperature effects. Regression analysis revealed a 6-month lag between the ONI and the global 11-month running UAH temperature. Trenberth and Fasullo [17] have used a 3-month lag in applying GISTEMP data without showing any analysis. Ollila [58] has used a parameter value of 0.144°$CONI^{-1}$ in transforming monthly ONI values into global temperature changes. Foster and Rahmstorf [62]

analyzed the magnitude of this coefficient in respect to the Multivariate El Niño Index (MEI) [63] and they found that the value is about 0.8 in respect to GISTEMP and about 1.4 to UAH temperature. The regression analysis was carried out between the ONI values and the 11-month running mean temperature values, the best choice was

$$dT_{ENSO} = 0.1 * ONI \quad (9)$$

Eq. (9) has been used in the both models. The transformation coefficient is the same as used by Trenberth and Fasullo [17]. It should be noticed that the global temperature impacts of ENSO events are based on empirical data. Therefore, this relationship includes the short-term positive water feedback.

Pacific Decadal Oscillation (PDO) has two general periodicities of 15-20 years and 50-70 years [64] and therefore PDO may have caused cooling or warming during the pause. The temperature effects of PDO and ENSO are almost identical [24,25] and therefore PDO effects are not considered in this study. The temperature effects of AMO [64] are restricted to estimating the temperature changes in the North Atlantic Ocean and therefore the AMO impacts are not considered in this study.

2.2.5 Cloudiness change temperature impacts

Changes in cloudiness also produce temperature effects through the GH (greenhouse) phenomenon. In its fourth assessment report [47], IPCC writes: "*Much of this thermal radiation emitted by the land and ocean is absorbed by the atmosphere, including clouds, and reradiated back to Earth. This is called the greenhouse effect.*" Increasing cloudiness increases surface temperature through the greenhouse effect but at the same time decreases incoming solar irradiation and therefore cloudiness changes have two opposite impacts on surface temperature.

Kauppinen et al. [57] and Ollila [65] have come to the same result using different analysis methods that the net cloud forcing in the interannual time scale can be calculated by a simple equation

$$dT_{CLOUD} = - 0.11 * CL\text{-}\% \quad (10)$$

Eq. (10) has been used to include the cloudiness change effects on the GSTM in the Ollila model.

3. RESULTS

3.1 Flux Values during the Pause

The first analysis depicts Total Solar Irradiance (TSI) and SW and LW flux values from 2000 to 2018 in Fig. 4. The SW flux value is the difference between the TSI/4 and the SW up flux caused by the albedo of the Earth. The LW flux up depends mainly on the surface temperature of the Earth, which is the result of SW flux at the surface and LW down flux at the surface. Therefore, LW flux up includes all the forcing elements of GH gases and other fluxes causing perturbations in the GH effect.

Because CERES flux values include seasonal variation, centered running averaging (CRA) methods have been applied. In this way the seasonal variation can be eliminated, and the results are 12-month runningmean values from January 2001 to June 2018 in Fig. 4.

The graphs in Fig. 4 reveal several notable features. About 99.97% of the total energy maintaining the Earth's temperature originates from the Sun. The TSI value has been changing according to the solar cycle, and its trend has been slightly declining. However, SW and LW radiation have increasing trends from 2000 to July of 2017, and thereafter these radiation fluxes have been rapidly descending, but they are still at a higher level than in the beginning of the pause. TSI variation is only 0.1%, but variation in SW radiation is 0.7%, from 240.75 to 241.93 Wm^{-2}. As clearly observed in Fig. 4, there is no correlation between TSI and SW radiation fluxes, which means that SW radiation changes or anomalies are probably due to the albedo changes of the Earth. The linear trend lines of SW and LW fluxes show that the RF of SW net forcing has been steadily increasing during the pause, and there is a clear positive RF value at the end of 2018.

3.2 Model Outputs during the Pause

The calculated SW change temperature effect has been normalized so that its average value for 2003–2014 is the same as the average value of UAH temperature change during the same period in the Ollila model, and analogously SW change temperature effect according to the IPCC model normalized to GISTEMP temperature. Both UAH and GISTEMP temperatures have been

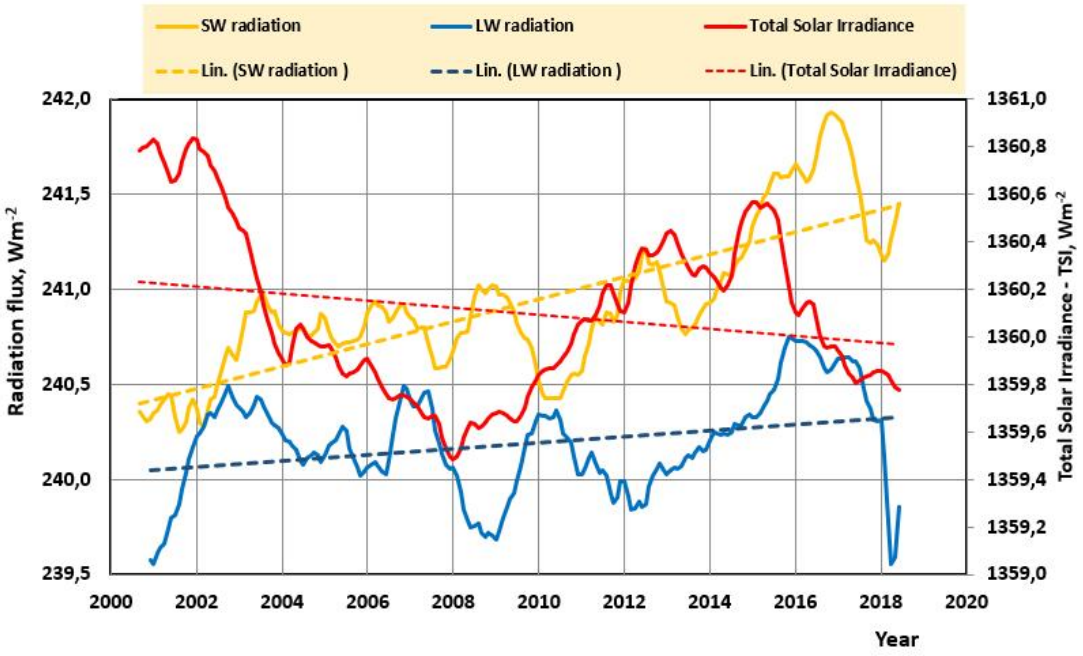

Fig. 4. The centered 12-month running mean values of TSI, SW and LW fluxes at the TOA including linear trend lines

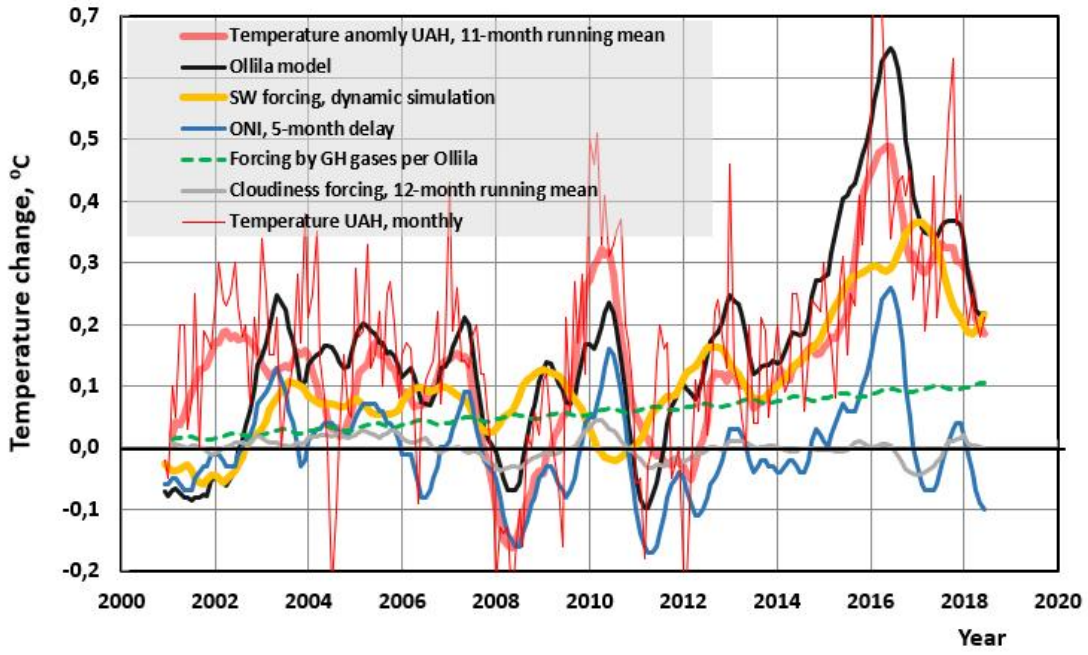

Fig. 5. Temperature effects of net radiative forcing factors according to the Ollila model

normalized to be zero at the end of 2000 as well as the GH gas effects and the RF effects of the IPCC model. The ONI has been applied as it is reported.

Fig. 5 depicts the temperature effects of the sum of the ONI, the cloud forcing, and the net SW forcing by simulation according to the Ollila model (Eq. (3)).

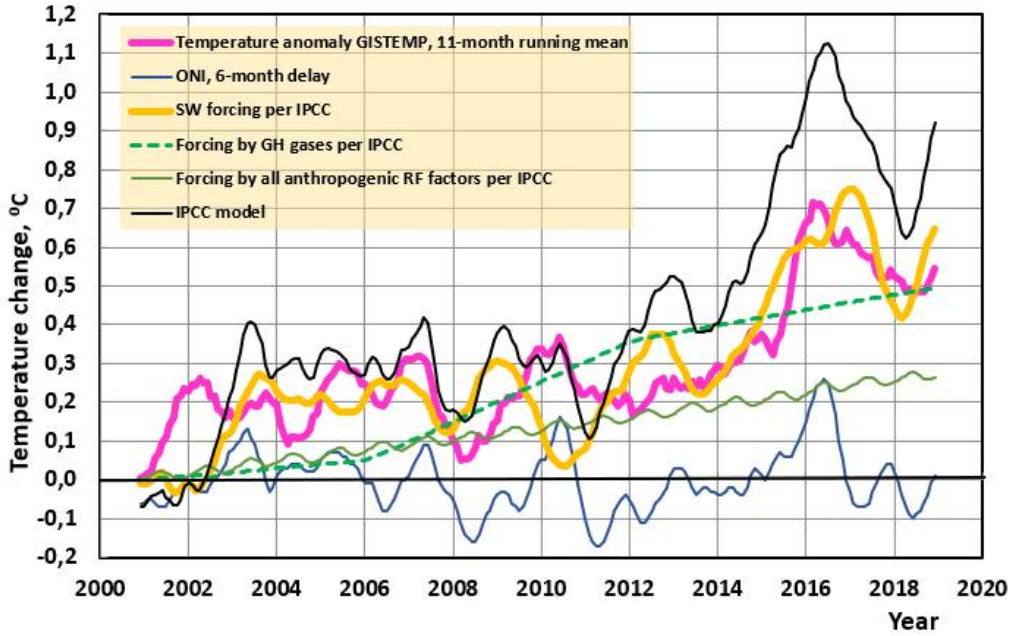

Fig. 6. Temperature effects of net radiative forcing factors according to the IPCC model

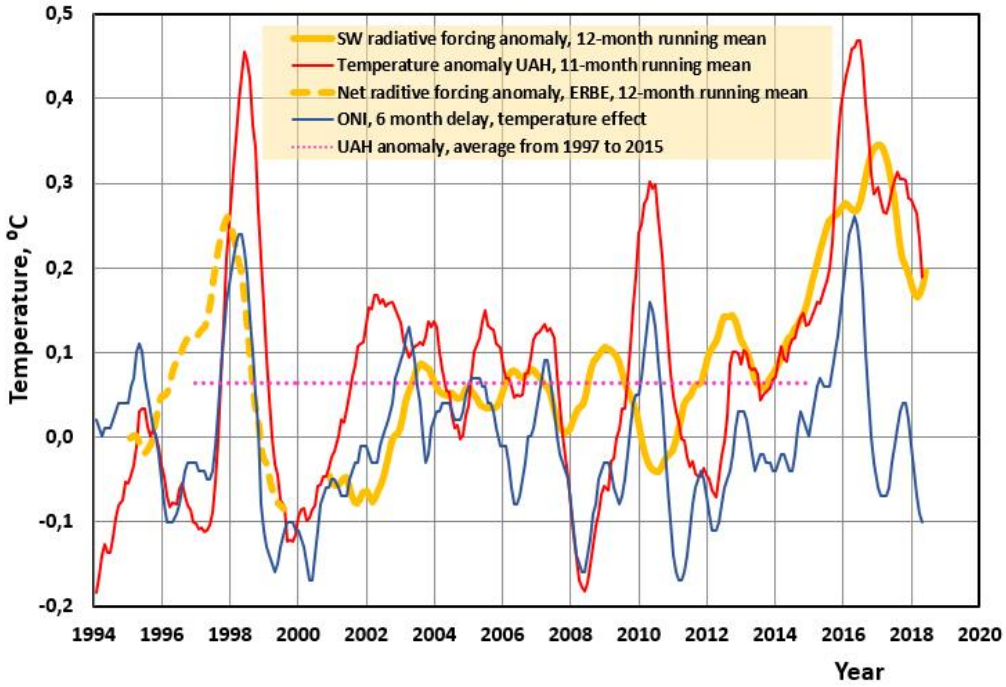

Fig. 7. Net global radiative fluxes are depicted according to ERBE [66] and CERES [52] data

ENSO temperature impacts during El Niño and La Niña can be clearly observed. The linear trend line of the ONI temperature impact during the pause is practically zero, as it should be in the long run, because ENSO events do not add long-term warming energy into the climate. The positive UAH trend is depending on the net SW forcing and the radiative forcings of GH gases.

It is easy to see from the graphs in Fig. 5 that the temperature of the Ollila model follows the UAH temperature. The temperature effects of cloudiness changes are very small: +0.046°C during El Niño 2010 and -0.045°C during El Niño 2015-16. Anyway, these impacts correct the model-calculated temperature in the right direction in comparison to the observed value.

The radiative forcings according to the IPCC models (Eq. (4)) are depicted in Fig. 6 together with the GISTEMP temperature anomaly graph.

The addition of aerosols and cloud effects into the total anthropogenic RF value decreases the IPCC model value dramatically. It should be noticed that according to the IPCC, the confidence levels for the RF values of CO_2, CH_4 and N_2O are very high or high, but the confidence levels for the RF values of aerosols and clouds are high and low respectively. This is not easy to understand, because direct aerosol observations are still under development, and there were no observations of these variables from 1750 up to about 1980.

The accuracy of the simple IPCC climate model can be compared to the three-dimensional CESM (Community Earth System Model) used by Trenberth et al. [40]. The error in the simulation between the observed and the CESM-calculated temperature value was 0.12°C - 0.4°C = -0.28°C at the end of 2014. The error between the GISTEMP and the IPCC model temperature of this study without SW impacts for the same period was -0.22°C showing that the difference between the models is small.

A good key figure for indicating the estimation accuracy of a model is the Mean Absolute Error (MAE). In this case the MAE is a mean value of absolute monthly differences between model values and observations. The MAE value for the Ollila model is 0.075°C in respect to UAH and 0.082°C in respect to GISTEMP. The MAE values of the IPCC model are respectively 0.191°C and 0.128°C. It means that the Ollila model estimates the observations with better accuracy. The coefficient of determination r^2 of the Ollila model with the UAH temperature is 0.676 and the same with the GISTEMP is 0.732.

Because it was found that the SW radiation has a major impact on the temperature increase during the super El Niño 2015-16, analyses were expanded to an earlier period from 1993 to 2000, during which the super El Niño 1997-98 happened. The radiation fluxes for this period are available from NASA's ERBE information. Actually, the readily calculated net radiation flux data of Fig. 7 by Wong et al. [66] was utilized. The net radiation fluxes of ERBE and CERES together with the ONI index and UAH temperature trends are depicted in Fig. 7.

The net flux anomalies of ERBE impacts are calculated with respect to the 1985–1989 period and the net flux anomalies of CERES have been calculated with respect to the 2001–2017 period. It can be noticed that also during the super El Niño 1997-98, the SW forcing has about the same warming effect as the ONI (the original El Niño effect). The conclusion is that in very strong (super) ENSO events, SW anomalies have a major effect on the global temperature. During weaker ENSO effects this phenomenon cannot be identified.

A more accurate analysis reveals that the SW forcing peak has its maximum value about 6 months before the El Niño temperature peak. This happened in connection with the El Niño peaks of 1997-98 and 2015-16. In 2010 a strong El Niño happened. Otherwise, as in the super El Niño, the SW forcing peak was in the opposite phase downwards. This situation may have been a reason why the strong El Niño in 2010 never developed into a super El Niño.

There is a decisive difference between the ENSO events of 1997-98 and 2015-16. La Niña was strong and long from June 1998 to December 2002 after the very strong El Niño. Two peaks of La Niña exceeded the strong definition limit. At the same time, SW forcing was at a very low level. After the super El Niño 2015-16 there was no strong La Niña but only two small peaks (2016 and 2017) reaching the low limit definition. This time SW forcing stayed at a very high level during these two La Niñas, which may be a reason for this situation. These findings show that SW forcing is an important climate event amplifier when it happens with an ENSO event being in the same phase. On the other hand, there is no answer so far as to why a SW anomaly happens sometimes in the same directions with both ENSO phases amplifying the temperature effects, like in 1997-98 and 1998-2002 and sometimes in the opposite phase, like El Niño 2010 or La Niña events in 2016-17.

Niño3.4 is the most sensitive area of the ENSO event, and it is a relatively small area in the region bounded by 5°N to 5°S, from 170°W to

120°W. The ONI is the three-month running average value of the sea-surface temperature anomaly of this area. In order to find out the possible relationship between the SW radiation flux and cloudiness, these entities in the Niño3.4 area have been depicted in Fig. 8a and the same global entities in Fig. 8b. The trends illustrate that during the El Niño phase, the cloudiness increases strongly, which has a strong negative effect on SW radiation in the Niño3.4 area.

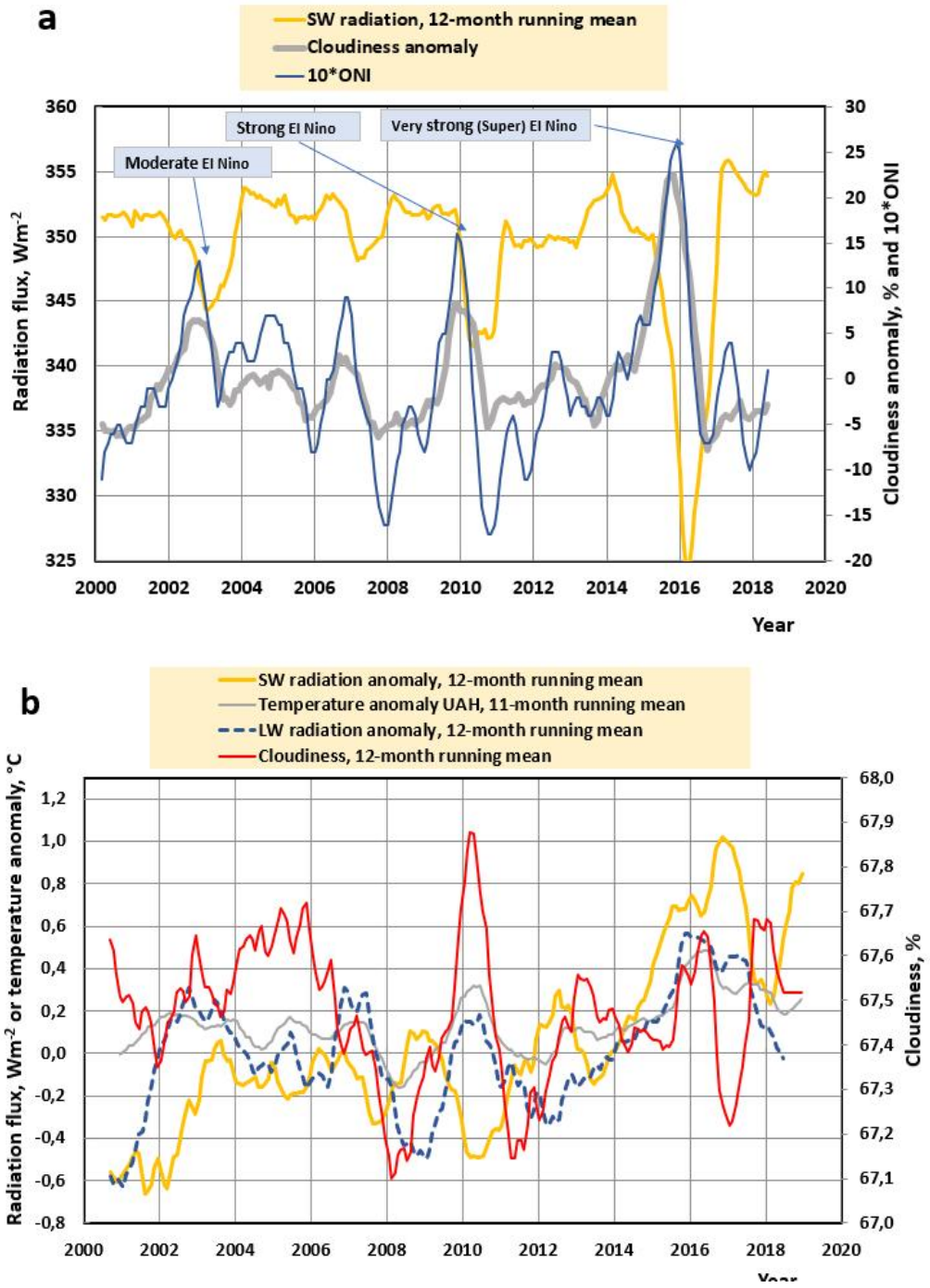

Fig. 8. (a). The SW flux, cloudiness and ONI trends at the Niño3.4 area (b). The global SW flux anomaly, LW flux anomaly, cloudiness, and temperature trends

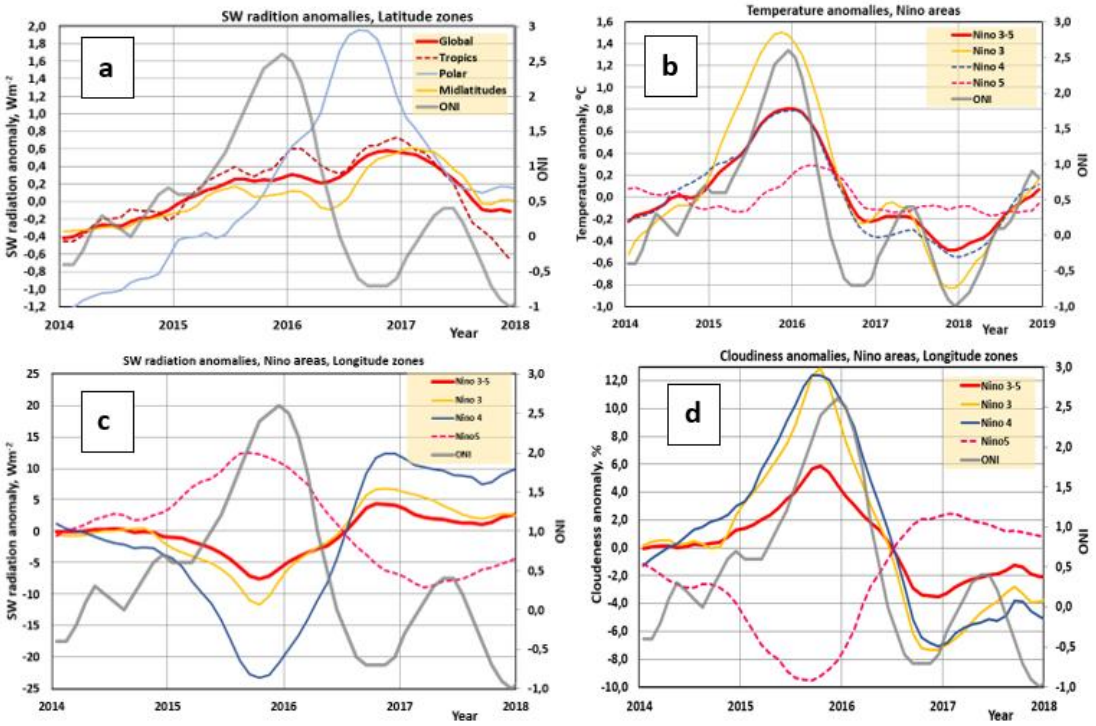

Fig. 9. (a). SW radiation anomalies in climate zones(b). Temperature anomalies in Niño areas (c). SW radiation anomalies in Niño areas (d). Cloudiness anomalies in Niño areas

The reason for the strong cloudiness increase is a great water evaporation rate, which has a global effect in the increasing absolute water vapor value in the whole atmosphere during the ENSO events (Figs. 2 and 3). In the Niño3.4 area there is a strong anti-correlation between the ONI and the cloudiness, the coefficient of correlation is 0.69, and the same between the ONI and the SW anomaly is -0.49, but the same globally is nonexistent 0.036.

For analyzing the possible relationship between the SW radiation flux, cloudiness and temperatures, these entities have been depicted in Fig. 9. The Niño areas in Fig. 9 are Niño 3 (90°W - 150°W), Niño 4 (150°W - 30°E), and Niño 5 (30°E - 90°E) having latitude limits of 5°N to 5°S. Niño 5 is not the official area definition, but a definition used in this study.

Fig. 9a shows that SW radiation anomalies during El Niño 2015-16 have about the same magnitude in tropics and midlatitudes but in the polar cap, the magnitude is much higher. According to Fig. 9b, 9c, and 9d the SW radiation, temperature, and cloudiness anomalies happen simultaneously in Niño 3 and 4. Cloudiness anomalies are positive during El Niño 2015-16 in Niño 3 and 4 but negative in Niño 5.

Loeb et al. [44] have carried out encompassing analyses between the cloud data of CERES [25] and the SW anomalies and they found that the correlation was 0.66 between the global SW anomalies and low level cloud variations that supports the cause-and-effect mechanism.

Cloudiness seems to vary independently, and it may have a role in amplifying SW anomalies and finally also a connection to the development of a super El Niño in a global scale. The mechanism and process of SW anomaly during the super El Niño are not known, and therefore it is too early to conclude what is the cause and effect relationship.

These analyses do not reveal a possible mechanism between the global SW flux anomalies and the ENSO events, because the global SW flux functions in the opposite ways during El Niño 2010-11 and 2015-16. During El Niño 2010, the SW anomaly was negative, and the cloudiness anomaly was positive (monthly maximum 68.5 %), and during El Niño 2015-15,

the SW anomaly was positive, and the cloudiness anomaly was negative (monthly minimum 65.9%). The question is whether it is a pure coincidence. Because there is an SW radiation flux upward anomaly during the El Niño 1997-98 and 2015-16, Bush et al. [67] have concluded that the SW anomaly in 1997-98 was caused by the ENSO event, but they have no analysis to support this claim. In Fig. 7 it can be noticed that just before super El Niño 1997-98 and 2015-16, SW radiation has reached its maximum value six months before the temperature maximum, and this extra energy may have triggered the super El Niño mechanism. The mechanism and process of SW anomaly during the super El Niño are not known and therefore it is too early to conclude what is the cause and effect relationship.

3.3 The End of the Pause

Because there was no strong or very strong La Niña after the super El Niño 2015-16 (as it should have been, like in the normal case after the super El Niño 1997-98), the question about the continuation of the pause of the 21stcentury has stayed open. From 2002 to 2014 there was practically no decreasing or increasing trend in GISTEMP and UAH temperatures. The super El Niño 2015-2016 started, according to the ONI, in November 2014 and ended in May 2016. Because the strong El Niño obscures other underlying climate forcing drivers – natural or anthropogenic – it has been challenging to define the actual ending point of the pause or even if it has ended at all. It was in October 2014 when the 11 months running GISTEMP overran the temperature of May 2010. Using the GSTM values as the only criteria for determining the pause endpoint, it would remove the ending point to somewhere around May 2016, when El Niño was over and the GSMT was still above the average pause temperature.

Trenberth et al. [40] concluded that the pause was still on at the end of 2015. Hu et al. [68] developed a simple climate model explaining the temperature changes from 1880 onward. They asserted that the higher temperatures of 2014-2016 ended the pause without considering that the GSMT could decrease rapidly after a super El Niño as it did after 1997-98. Their analysis also concluded that ENSO-related anomalous heating modulated GSMT, creating the pause. Actually, this explanation would mean that ENSO events created fewer heating effects in the 2000s than normally. By analyzing the magnitudes of ENSO events, this claim may be justified. This study introduces a new cause for this heating anomaly as can be seen in Fig. 7. There was an unusually deep and long La Niña from June 1998 to December 2002. At the same time, the SW radiation was at low levels, driving GSMT downwards.

Su et al. [69] carried out a detailed analysis of the real warming impacts of the super El Niño effects. Their conclusion was that El Niño provided only one-third of the total GSMT increase during 2015 and the pause was over around 2014.

The results of this study show that at the end of 2014, the portions of driving forces measured as temperature effects were SW forcing 45%, El Niño 40%, greenhouse gases 14% and clouds 1%. El Niño's portion of one-third as reckoned by Su et al. [69] is close to the 40% of this study. The SW forcing exceeded its maximum pause value of July-October 2012 in November 2014. A retrospective analysis shows that the pause was really over at the end of 2014 and this study introduces a new natural cause for the ending. This means that SW forcing is the major reason for the ending of the pause.

ENSO events are relatively short climate phenomena. In the long run, they do not act as climate drivers because the real climate drivers are anthropogenic drivers and cosmic forces like the sun.

4. DISCUSSION

The results of this study show that the simple and robust climate model of Ollila without positive water feedback explains the temperature changes during the pause with good accuracy. The most surprising new result is that the major contributor for the temperature increases of the super El Niño of 1997-98 and 2015-16 is not the natural El Niño effect but a SW anomaly impact. This is an alternative explanation for the mechanism suggested by Hong et al. [50] that Southern Hemispheric transverse circulation is a prerequisite for extreme magnitude El Niño events.

Both models include several components that have been treated as independent variables. The coefficients of determinations were between ONI and SW radiation 0.017, between cloudiness and SW radiation 0.017, and between ONI and cloudiness 0.37. This last correlation may have

effects on the results. Ollila model without cloud impacts did not improve the overall key figures but the MAE in respect to UAH increased from 0.075°C to 0.081°C and the coefficient of determination decreased from 0.676 to 0.626. The absolute temperature effects of cloudiness changes are very small, but they have an improving effect on the model output.

In the Niño3.4 area during El Niño 2010 and 2015-16, the SW radiation anomaly was negative due to the strong positive cloudiness anomalies. On the global scale, cloudiness and SW anomalies were also in the same phases, but during El Niño 2010, the SW anomaly was negative, and the cloudiness anomaly was positive, and during El Niño 2015-15, the SW anomaly was positive, and the cloudiness anomaly was negative. It is logical that increased cloudiness decreases SW radiation. It is not straightforward to conclude the cause-and-effect relationship in this case. It is more probable that cloudiness changes first and it causes a SW anomaly than otherwise. The general reasons for cloudiness changes are still unknown.

As depicted in Fig. 8, the SW radiation anomaly is strongly negative in the Niño3.4 area during the super El Niño, and at the same time it may be significantly positive on a global scale like in 2015–16. This finding—that the regional and global effects may be totally opposite at the same time regarding forcing impacts or forcing magnitudes—is not new [40,70]. A common explanation for the global effects of regional ENSO events is a teleconnection mechanism [71]. The SW anomalies related to very strong ENSO events provide another explanation.

The prevailing explanation of the global warming is the same as the scientific results of the IPCC reports [47-49]: The reasons are anthropogenic, which are mainly due to the increased concentrations of GH gases. In the latest assessment report AR5 [48], the RF value of anthropogenic forcing elements is 2.29 Wm^{-2}, which is 97.9% of the total RF of 2.34 Wm^{-2}. The results of the two models (IPCC model and Ollila model) show that there is a significant difference between the anthropogenic forcing values: 0.1°C versus 0.26°C at the end of the pause.

The UAH temperature in from July 2017 to July 2018 was about 0.19°C above the average value for 2002–2014 and the GISTEMP was about 0.3°C above the pause average. The question about the continuation of the pause has been under debate. The conclusion of this study is that the pause was over at the end of 2014, but the major cause was not the anthropogenic forcing: it was the SW radiation forcing.

There are alternative theories for the global warming, including cosmic forces.Svensmark [72] theorizes that cosmic radiation magnifies solar insolation changes through cloudiness. Ermakov et al. [73] and Scafetta [74] have introduced the theory of Astronomical Harmonic Resonances (AHR) having a 60-year main cycle. Ollila [62] has combined the Sun theory, AHR, and anthropogenic impacts in the Semi-Empirical Climate Model (SECM), which can explain the temperature changes since 1630 with the coefficient of correlation at 0.90. In the SECM during the pause, the temperature impact of GH gases is +0.1°C and the same of AHR is -0.04°C, which means a negligible summary effect of 0.06°C. This result fits very well into the Ollila model-calculated temperature effects, suggesting that the SW anomalies and ENSO events have major roles in temperature changes during the pause.

A common feature in these cosmic theories is that the influence mechanism of the solar insolation changes as well as AHR changes happens through the cloudiness changes. In Fig. 8b, the global cloudiness anomaly and SW anomaly trends are depicted. During the 2010 El Niño, the cloudiness has a strong anomaly downward both globally and at the Niño3.4 area. During the 2015-16 El Niño, the cloudiness has a downward anomaly globally but an upward anomaly at the Niño3.4 area. There is no logical explanation for this phenomenon. The 1% cloudiness change causes a 0.1°C temperature change according to two studies [57,65]. The temperature impact of the cloudiness change can explain only about 10 % of the temperature effect of the SW anomaly during the pause.

A more accurate explanation for the temperature effect of cloudiness changes comes from the recent findings of Loeb et al. [40] that show that SW radiation changes correlate to low level clouds. A further explantation could be that the low-level clouds actually correlate to cosmic radiation changes much better than to over-all cloudiness changes [75]. According to Svensmark [72] the atmosphere modulates the incoming solar radiation in a significant way through albedo changes. This study shows that the change of albedo from 29.4% to 28.9% has caused 0.26°C maximum change during the

pause if the SW changes are caused by the albedo changes. The albedo of the Earth depends on three reflected radiation fluxes, which form the total albedo: clouds 64.0%, surface 22.7% and atmosphere 17.4% [76]. The surface albedo has probably remained constant. Cloudiness is changing all the time, and it is an imminent contributor for short- and long-term albedo changes, but there may be other unknown factors in the atmosphere causing albedo changes.

5. CONCLUSIONS

A simulation of the simple Ollila model combining the SW effects, ENSO effects, GH effects and cloud effects with no water feedback (λ=0.27 K/(Wm^{-2})) follows the real UAH temperature changes with the mean absolute error (MAE) of 0.073°C and the GISTEMP with 0.082°C. This result means that during the pause, there is no long-term positive water feedback. The mean absolute error of the IPCC model with positive water feedback is 0.128°C in respect to the GISTEMP and 0.191°C in respect to the UAH. Positive water feedback seems to be the major reason for the error, which amplifies both SW forcing and anthropogenic forcing values by a factor of about 100% in comparison to the Ollila model.

Along with ENSO events, net SW radiation changes have dominated the temperature changes during the pause of the 2000s. Especially during the super El Niño of 2015-16, SW radiation anomaly had a greater impact than the original El Niño warming effect, and the same effect can be observed during the super El Niño 1997-98. The increasing absolute water vapor value in the atmosphere should mean higher global cloudiness during the El Niño phases, but cloudiness trends show that in some cases, such as during the super El Niño 2015-16, the opposite may happen. These contradictions mean that atmospheric processes still need basic scientific research work.

The results mean that about the half of the global temperature changes during the super El Niño events are due to the SW radiation changes. The other half of the changes are due to the original ENSO impacts. The global water vapor changes originating from ENSO effects account for about 50 % of the global temperature changes that are due to ENSO effects.

SW radiation changes do not correlate with the solar cycle insolation changes, but the SW perturbations are very probably due to the albedo changes in the atmosphere. There is a weak correlation to cloudiness anomalies, but they cannot explain the overall changes during the pause.

The UAH temperature of 2018 was about 0.15°C above the average value for 2002–2014, the GISTEMP was about 0.27°C above the pause average, and the SW forcing was 0.24°C during the year 2018. The conclusion of this study is that the pause was over at the end of 2014, and the major cause was not the anthropogenic forcing, but it was the SW radiation forcing. The present high temperatures from 2017 to 2020 are very probably due to the positive SW radiation anomaly. If SW radiation forcing happens during a relatively short period of time, any factors causing SW perturbations may have an even greater role in the long-term changes. The IPCC has concentrated on anthropogenic climate change issues, but more efforts should be used for research to find different factors causing changes in the Earth's albedo.

An interesting result of this study is that the simple IPCC climate model gave almost the same warming for the period 2000-2014 as the complicated 3-dimensional Community Earth System Model (CESM) in the paper of Trenberth et al. [40]. The obvious reason is in the same physical warming model for anthropogenic climate drivers in both models.

COMPETING INTERESTS

Author has declared that no competing interests exist.

REFERENCES

1. Knight J. Global oceans. Do global temperature trends over the last decade falsify climate predictions? Bull. Am. Meteorol. Soc. 2009;90:S56-S57.
2. Fyfe JC, Meehl GA, England MH, Mann ME, Santer BD, Flato GM, Hawkins E, Gillett NP, Xie S-P, Kosaka Y, Swart NC. Making sense of the early-2000s warming slowdown. Nat. Clim. Change. 2016;6:224–228.
3. Otto A, Otto FEL, Boucher O, Church J, Hegerl G, Forster PM, Gillett NP, Gregory J, Johnson GC, Knutti R, Lewis N, Lohmann U, Marotzke J, Myhre G, Shindell D, Stevens B, Allen MR. Energy budget constraints on climate response. Nat. Geosci. 2013;6:415-416.

4. Fyfe JC, Gillett NP, Zwiers FW. Overestimated global warming over the past 20 years Nat. Clim. Change. 2013;3:767–769.
5. Kerr R.What happened to global warming? Scientists say just wait a bit. Science. 2009;326:28–29.
Available:https://doi:101126/science326_28a
6. Hunt BG. The role of natural climatic variation in perturbing the observed global mean temperature trend. Clim. Dyn. 2011;36:509–521.
Available:https://doiorg/101007/s00382-010-0799-x
7. Meehl GA, Arblaster JM, Fasullo JY, Hu A, Trenberth KE. Model-based evidence of deep-ocean heat uptake during surface-temperature hiatus periods. Nature Clim. Change. 2011;1:360-364.
8. Schmidt GA, Shindell DT, Tsigaridis K. Reconciling warming trends. Nat. Geosci. 2014;7:158–160.
9. Huber M, Knutti R. Natural variability radiative forcing and climate response in the recent hiatus reconciled. Nat. Geosci. 2014;7:651–656.
10. Risbey JS, Lewandowsky S, Langlais C, Monselesan DP, O'Kane TJ, Oreskes N. Well-estimated global surface warming in climate projections selected for ENSO phase. Nat. Clim. Change. 2014;4:835–840.
11. Lewandowsky S, Risbey JS, Oreskes N. On the definition and identifiability of the alleged 'hiatus' in global warming. Sci. Rep. 2015;5:16784.
12. Lin M, Huybers P. Revisiting whether recent surface temperature trends agree with the CMIP5 ensemble. J. Clim. 2016;29:8673–8687.
Available:https://doiorg/101175/JCLI-D-16-01231
13. Katsman CA, van Oldenborgh GJ. Tracing the upper ocean's missing heat. Geophys. Res. Lett. 2011;38:L14610.
Available:https://doiorg/101029/2011GL048417
14. Meehl GA, Teng H. Case studies for initialized decadal hindcasts and predictions for the Pacific region. Geophys. Res. Lett. 2012;39:L22705.
Available:https://doiorg/101029/2012GL053423
15. Palmer MD, McNeall DJ, Dunstone NJ. Importance of the deep ocean for estimating decadal changes in Earth's radiation balance. Geophys. Res. Lett. 2011;38:L12707.
Available:https://doiorg/101029/2011GL047835
16. Guemas V, Doblas-Reyes FJ, Andreu-Burillo I, Asif M. Retrospective prediction of the global warming slowdown in the past decade. Nat. Clim. Change. 2013;3:649–653.
17. Trenberth KE, Fasullo JT. An apparent hiatus in global warming? Earth's Future. 2013;1:19–32.
Available:https://doiorg/101002/2013EF000165
18. Smith DG. Oceanography: Has global warming stalled? Nat. Clim. Change. 2013;3:618–619.
19. Chen X, Tung KK. Varying planetary heat sink led to global-warming slowdown and acceleration Science. 2014;345:897–903.
Available:https://doi:101126/science1254937
20. Durack PJ, Gleckler PJ, Landerer FW, Taylor KE. Quantifying underestimates of long-term upper-ocean warming. Nat. Clim. Change. 2014;4:999–1005.
21. Yan XH, Bouyer T, Trenberth KE, Karl TR, Xie S-P, Nieves V, Tung K-K, Roemmich D. The global warming hiatus: slowdown or redistribution? Earth's Future. 2016;4:472–482.
Available:https://doiorg/101002/2016EF000417
22. Cheng L, Trenberth KE, Fasullo JT, Mayer M, Balmaseda M, Xhu J. Evolution of ocean heat concent related to ENSO. J. Climate. 2019;32:35293556.
23. Kosaka Y, Xie SP. Recent global-warming hiatus tied to equatorial pacific surface cooling. Nature. 2013;501:403-407.
24. National Center for Atmospheric Research (NCAR). PDO index.
Available:https://climatedataguideucaredu/climate-data/pacific-decadal-oscillation-pdo-definition-and-indices
25. National Center for Atmospheric Research (NCAR). AMO index.
Available:https://climatedataguideucaredu/climate-data/atlantic-multi-decadal-oscillation-amo
26. Hansen J, Sato M, Kharecha P, von Schuckmann K. Earth's energy imbalance and implications. Atmos. Chem. Phys. 2011;11:13421-13449.
Available:https://doiorg/105194/acp-11-13421-2011

27. Solomon S. Contributions of stratospheric water vapor to decadal changes in the rate of global warming. Science. 2010;327: 1219-1223.
Available:https://doi101126/science1182488
28. Solomon S. The persistently variable 'background' stratospheric aerosol layer and global climate change. Science. 2011;333:866-870.
Available:https://doi101126/science1206027
29. Santer BD, Bonfils C, Painter JF, Zelinka MD, Mears C, Solomon S, Schmidt GA, Fyfe JC, Cole JNS, Nazarenko L, Taylor KE, Wentz FJ. Volcanic contribution to decadal changes in tropospheric temperature.Nat. Geosci. 2014;7:85-189.
30. Brohan P, Kennedy JJ, Harris I, Tett SFB, Jones PD. Uncertainty estimates in regional and global observed temperature changes: A new dataset from 1850. J. Geophys. Res. Atmos. 2006;111:D12106.
Available:https://doiorg/101029/2005JD006548
31. Easterling DR, Wehner MF. Is the climate warming or cooling? Geophys. Res. Lett. 2009;36:L08706.
Available:https://doiorg/101029/2009GL037810
32. Hansen J, Ruedy R, Sato M, Lo K. Global surface temperature change. Rev. Geophys. 2010;48:RG4004.
Available:https://doiorg/101029/2010RG000345
33. Foster G, Rahmstorf S. Global temperature evolution 1979–2010. Environ. Res. Lett. 2011;6:044022.
Available:https://doi:101088/1748-9326/6/4/044022
34. Kaufmann RK, Kauppi H, Mann ML, Stock JH. Reconciling anthropogenic climate change with observed temperature 1998–2008. Proc. Nat. Acad. Sci. USA. 2011;208:11790–11793.
Available:https://doiorg/101073/pnas1102467108
35. Cohen JL,Furtado JC, Barlow M, Alexeev VA, Cherry JE. Asymmetric seasonal temperature trends. Geophys. Res. Lett. 2012;39:L04705.
Available:https://doiorg/101029/2011GL050582
36. Cowtan K, Way RG. Coverage bias in the HadCRUT4 temperature series and its impact on recent temperature trends. Q. J. R. Meteorol. Soc. 2014;140:1935-1944.
Available:https://doi:101002/qj2297
37. Rajaratnam B, Romano J, Tsiang M, Diffenbaugh NS. Debunking the climate hiatus. Climatic Change. 2015;133:129–140.
Available:https://doi:101007/s10584-015-1495-y
38. Karl TR, Arguez A, Huang B, Lawrimore JH, McMahon JR, Menne MJ, Peterson TC, Vose RS, Zhang HM. Possible artifacts of data biases in the recent global surface warming hiatus. Science. 2015;348(6242):1469–1472.
Available:https://doi:101126/scienceaaa5632
39. Lewandowsky S, Risbey JS, Oreskes N. The 'pause' in global warming: turning a routine fluctuation into a problem for science. Bull. Am. Meteorol. Soc. 2016;97: 723–733.
Available:https://doiorg/101175/BAMS-D-14-001061
40. Trenberth KE, Zhang Y, Fasullo JT. Relationships among top-of-atmosphere radiation and atmospheric state variables in observations and CESM. J. Geophys. Res. Atmos. 2015;120:10074–10090.
Available:https://doiorg/101002/2015JD023381
41. Scafetta N, Mirandola A, Bianchini A. Natural climate variability part 2: Interpretation of the post 2000 temperature standstill. I.J.H.T. 2017;35:S18-S26.
Available:https://doi:1018280/ijht35Sp0103
42. Yin J, Overbeck J, Peyser C, Stouffer R. Big jump of record warm global mean surface temperature in 2014-2016 related to unusually large oceanic heat releases. Geophys. Res. Lett. 2018;45:1069-78.
43. Hedemann C, Mauritsen T, Jungclaus J, Marotzke J. The subtle origins of surface-warming hiatuses. Nat. Clim. Change. 2017;7:336–339.
44. Loeb NG, Thorsen TJ, Norris JR, Wang H, Su W. Changes in earth's energy budget during and after the "pause" in global warming: An observational perspective. Climate. 2018;6:62.
DOI: 103390/cli6030062
45. The University of Alabama in Hunsville (UAH). UAH temperature dataset.
Available:https://wwwnsstcuahedu/data/msu/v60/tlt/uahncdc_lt_60txt

46. National Oceanic and Atmospheric Adminsitration (NOAA). GISS surface temperature analysis (GISTEMP). Available:https://datagissnasagov/gistemp/
47. IPCC AR4. Summary for Policymakers. IPCC Fourth assessment report of the Intergovernmental Panel on Climate Change. Cambridge University Press, Cambridge, UK; 2007.
48. IPCC AR5. The fifth assessment report. The physical science basis working group I contribution to the IPCC fifth assessment report of the Intergovernmental Panel on Climate Change. Cambridge University Press, Cambridge, UK; 2013.
49. IPCC TAR. The third assessment report Climate Change 2001. The Scientific basis Cambridge University Press, Cambridge, UK; 2001.
50. Hong LC, Lin HO, Jin FF. A southern hemisphere booster of super El Niño. Geophys. Res. Lett. 2014;41:2142-2149. Available:https://doiorg/101002/2014GL059370
51. National Oceanic and Atmospheric Adminstration (NOAA). Oceanic Niño Index (ONI). Available:https://wwwnwfscnoaagov/research/divisions/fe/estuarine/oeip/cb-meicfm
52. National Oceanic and Atmospheric Adminstration (NOAA). CERES EBAF-TOA Data Products. Available:https://ceres-toollarcnasagov/ord-tool/jsp/EBAF4Selectionjsp
53. National Oceanic and Atmospheric Administration (NOAA)NCEP/NCAR Reanalysis Data. Available:https://wwwesrlnoaagov/psd/cgi-bin/data/timeseries/timeseries1pl (Accessed on 9 January 2019)
54. National Oceanic and Atmospheric Administration (NOAA). NOAA's annual greenhouse index. Available:https://wwwesrlnoaagov/gmd/aggi/
55. Ollila A. Challenging the scientific basis of the Paris climate agreement. Int. Jl. Clim. Ch. Man. 2018;11(1):18-34. Available:https://doiorg/101108/IJCCSM-05-2017-0107
56. Stine AR, Huybers P, Fung IY. Changes in the phase of the annual cycle of surface temperature. Nature. 2009;457:435-441.
57. Kauppinen J, Heinonen JT, Malmi PJ. Major portions in climate change: Physical approach. Int. Rev. Phys. 2011;5:260-270.
58. Ollila A. Climate sensitivity parameter in the test of the Mount Pinatubo eruption. Ph. Sc. Int. Jl. 2016;9(4):1-14.
59. Ollila A. The potency of carbon dioxide (CO_2) as a greenhouse gas. Dev. in Earth Sc. 2014;2:20-30.
60. Ollila A. Warming effect reanalysis of greenhouse gases and clouds. Ph. Sci. Int. Jl. 2019;13:1-13.
61. Ollila A. Challenging the greenhouse effect specification and the climate sensitivity of the IPCC. Ph. Sc. Int. Jl. 2019;22(2):1-19.
62. Foster AG, Rahmstorf S. Global temperature evaluation 1979-2010. Environ. Res. Lett. 2011;6:1-8.
63. National Oceanic and Atmospheric Administration (NOAA). MEI index. Available:https://wwwesrlnoaagov/psd/enso/mei/
64. Mantua NJ, Hare SR. The Pacific decadal oscillation. J. Oceanogr. 2002;58:35–44.
65. Ollila A. Dynamics between clear cloudy and all-sky conditions: cloud forcing effects. J. Chem. Biol. Phys. Sc. 2013;4: 557-575.
66. Wong T, Wielicki BA, Lee III RB, Smith LS, Bush KA, Willis JK. Reexamination of the Observed Decadal Variability of the Earth Radiation Budget Using Altitude-Corrected ERBE/ERBS Nonscanner WFOV Data. J. Clim. 2005;19:4028-4040. Available:https://doiorg/101175/JCLI38381
67. Bush KA, Smith GL, Lee RB, Young DF. The Earth Radiation Budget Experimetn (ERBE) 15-year data set. Proc. SPIE. 2003;4888. Remote Sensing Clouds and the Atmosphere VII. Available:htpps://doi:101117/12463008
68. Hu S, Fedorov AV: The extreme El Niño of 2015-2016 and the end of global warming hiatus. Geophys. Res. Lett. 2017;44:3816-3824. DOI: 101002/2017GL072908
69. Su J, Zhang R, Wang H. Consecutive record-breaking high temperatures marked the handover from hiatus to accelerated warming. Sci. Rep. 2017;7:43735.
70. Brown PT, Li W, Jiang JH, Su H. Unforced surface air temperature variability and its contrasting relationship with the anomalous TOA energy flux at local and

global spatial scales. J. Climate. 2016;29:925–940.
Available:https://doiorg/101175/JCLI-D-15-03841

71. Yang S, Li Z, Yu JY, Hu X, Dong W, He S. El Niño–Southern Oscillation and its impact in the changing climate. Nat. Sc. Rev. 2018;5:840–857.
Available:https://doiorg/101093/nsr/nwy046
72. Svensmark H. Influence of cosmic rays on earth's climate. Phys. Rev. Lett. 1998;29(5):487–494.
Available:https://doiorg/101103/PhysRevLett815027
73. Ermakov V, Okhlopkov V, Stozhkov Y. Influence of cosmic rays and cosmic dust on the atmosphere and Earth's climate. Bull. Russ. Acad. Sc. Ph. 2009;73:434-436.
Available:https://doiorg/103103/S1062873809030411
74. Scafetta N. Empirical evidence for a celestial origin of the climate oscillations and its implications.J. Atmos. Sol. Terr. Phys. 2010;72:951-970.
DOI: 101016/jjastp201004015
75. Marsh ND, Svensmark H. Low cloud properties influenced by cosmic rays. Phys. Rev. Lett. 2000;85:5004-5007.
Available:https://doiorg/101103/PhysRevLett855004.
76. Ollila A. Earth's energy balance for clear cloudy and all-sky conditions. Dev. in Earth Sc. 2013;1:1-10.

Peer-review history:
The peer review history for this paper can be accessed here:
http://www.sdiarticle4.com/review-history/55149